

# Laser pulse amplification and dispersion compensation in an effectively extended optical cavity containing Bose-Einstein condensates

D Tarhan<sup>1</sup>, A Sennaroglu<sup>2</sup>, Ö E Müstecaplıoğlu<sup>2</sup>

<sup>1</sup>Harran University, Department of Physics, 63300, Şanlıurfa, Turkey

<sup>2</sup>Koç University, Department of Physics, 34450, Sarıyer, Istanbul, Turkey

E-mail: omustecap@ku.edu.tr

## Abstract.

We review and critically evaluate our proposal of a pulse amplification scheme based on two Bose-Einstein condensates inside the resonator of a mode-locked laser. Two condensates are used for compensating the group velocity dispersion. Ultraslow light propagation through the condensate leads to a considerable increase in the cavity round-trip delay time, lowers the effective repetition rate of the laser, and hence scales up the output pulse energy. It has been recently argued that atom-atom interactions would make our proposal even more efficient. However, neither in our original proposal nor in the case of interactions, limitations due to heating of the condensates by optical energy absorption were taken into account. Our results show that there is a critical time of operation, 0.3 ms, for the optimal amplification factor, which is in the order of  $\sim 10^2$  at effective condensate lengths in the order of  $\sim 50 \mu\text{m}$ . The bandwidth limitation of the amplifier on the minimum temporal width of the pulse that can be amplified with this technique is also discussed.

PACS numbers: 42.50.Gy

Submitted to: *J. Phys. B: At. Mol. Opt. Phys.*

## 1. Introduction

High peak-power laser pulses are sought in diverse scientific and technological applications such as biomedical imaging [1], ultrafast spectroscopy [2], and high harmonic generation [3]. Ultrashort laser pulses in the picosecond to femtosecond range are routinely produced by the technique of mode locking, where the axial modes of the cavity are locked in phase to produce a train of pulses with a repetition rate  $f_{\text{rep}} = c/2L$ , where  $c$  is the speed of light and  $L$  is the effective optical path length of the resonator [4]. Pulse energies directly generated from such lasers are typically in the nJ range and amplification schemes are necessary in order to scale up the peak intensities to levels where nonlinear interactions can be observed. Recently, a simple amplification method was demonstrated, based on the extension of the standard mode-locked resonator length with a compact multipass cavity [5]. If the added insertion loss of the extended cavity is negligible, the average output power of the laser remains nearly the same and extension of the cavity length scales up the energy per pulse by lowering the repetition rate. While this technique has been widely used to amplify femtosecond pulses up to  $\mu\text{J}$  energies [6], there is an ever growing need to find amplification methods that will facilitate the construction of even more compact, high-intensity lasers.

About five years ago, we proposed a compact laser pulse amplification scheme using two Bose-Einstein condensates (BECs) introduced in the resonator of a mode-locked laser [7]. The basic idea was to utilize the electromagnetically induced transparency (EIT) scheme [8, 9, 10, 11] in a cavity [12] to make the pulse ultraslow [13, 14] such that the effective pulse repetition rate could be drastically reduced due to the increase of the cavity round-trip time, provided that the average output power of the laser remains nearly the same after the introduction of the condensates, this increase in round-trip time then scales up the output energy.

The promise of laser pulse amplification by atomic condensates is further studied by taking into account atom-atom interactions in f-deformed condensate formalism very recently [15]. It is found that interactions make the amplification effect stronger. Moreover, in addition to subluminal propagation, possibility of superluminal speeds and high degree of control over the repetition rate are also shown to be possible. On the other hand, neither of these works consider the effects of the heating of the condensates due to optical pulse absorption. Present work is a critical evaluation of the feasibility of the proposal by taking into account the temperature increase of the condensates during pulse propagation.

In the design of a practical BEC pulse amplifier, certain effects need to be further considered. First, because the BEC would introduce an excessive amount of dispersion to short pulses [16], undesirable pulse broadening results. To overcome this limitation, we offer a method for dispersion compensation by using a second intracavity BEC with the proper choice of energy levels to provide the opposite sign of dispersion. Second BEC can be in fact prepared identical with the first, and a magnetic field can be utilized to shift the energy levels of the second BEC to match the desired detuning

of the probe pulse. Second, the transparency bandwidth of the EIT process puts a limitation on the shortest temporal pulsewidth that can be amplified in the resonator. Resulting bandwidth limitation of the amplifier is further discussed. Our results show that, pulse energy amplification factors of  $\sim 10^2$  are possible by using a  $^{23}\text{Na}$  BEC with effective lengths of  $\sim 10 - 100 \mu\text{m}$ . Finally, heating of the condensate, due to small but nonzero absorption in the EIT scheme, introduces an operational time beyond which the condensate turns into usual Maxwell-Boltzmann gas. Our calculations reveal a critical time, 0.3 ms, at which the amplification factor is optimum.

The significance of proposed method of effectively increasing the length of the cavity against the straightforward solution of extended cavities should be clarified. In fact it is of high demand to have compact laser cavities in practical laser systems. In applications like optical data storage, filtering or other optical logic and signal processing, having long optical paths, for long optical delay, while maintaining cavity volume small brings tremendous practical advantages. The search for such compact cavities goes back to mid 1960s. Herriott et al. introduced the method of folding long optical paths for compact cavities [17]. Around early 2000, multi-pass cavities were developed by Cho et al [5]. This is now an active modern research field (for a review see Ref. [18]). In ultraslow light scheme by electromagnetically induced transparency, optical pulses slow down to speeds about few meters/second. Thus the effective optical path is indeed too long for considering an equivalent extended cavity. In addition to the typical applications of compact laser cavities in accurate optical loss measurements, stimulated Raman scattering, long-path absorption spectroscopy, high-speed path-length scanning, present system of ultraslow light has another crucial application area of coherent optical memory. With modest amplification power and dispersion compensation, proposed scheme can also be used for that purpose in the context of correcting pulse shape errors in the stored optical information.

This paper is organized as follows. Method of generating ultraslow light via EIT scheme is introduced briefly in Sec. 2. We describe our proposed scheme in Sec. 3. The results of dispersion compensation, heating rate, amplification factor and spectral bandwidth calculations are presented in the corresponding subsections of Sec. 4. We conclude in Sec. 5.

## **2. Ultraslow light by EIT scheme**

In the EIT configuration, a condition of weak probe is usually assumed, such that, a strong drive field with Rabi frequency  $\Omega_c$  and the circulating resonator field of frequency  $\Omega_p$  satisfy  $\Omega_c \gg \Omega_p$  [19]. A conventional configuration is the case where the probe field is pulsed while the drive field is continuous wave (CW) [10]. Studies and experiments in the strong probe regime indicate deterioration of EIT and enhanced absorption of the probe pulse [20]. Requirements for initiation of EIT is formulated in terms of Rabi frequencies [21]. We are assuming that Rabi frequency of the amplified pulsed signal remains sufficiently smaller than the Rabi frequency of the cw drive so that the EIT conditions

are maintained during the operation. Our results reveal a maximum of amplification factor and the strength of the cw control field can be chosen accordingly. Though we did not specifically investigate it here, our scheme may also be used for compensating enhanced absorption in the strong probe EIT experiments. This would be particularly advantageous to examine interactions of probe and coupling fields [22], adiabats [23], as well as to facilitate nonlinear processes demanded for EIT applications [24, 25, 26, 27].

Under the weak probe condition, susceptibility  $\chi$  for the probe transition can be calculated as a linear response as most of the atoms remain in the lowest state. Assuming local density approximation, neglecting local field, multiple scattering and quantum corrections and employing steady state analysis,  $\chi$  is found to be [19]

$$\chi = \frac{\rho |\mu_{31}|^2}{\varepsilon_0 \hbar} \frac{i(-i\Delta + \Gamma_2/2)}{(\Gamma_2/2 - i\Delta)(\Gamma_3/2 - i\Delta) + \Omega_C^2/4}, \quad (1)$$

where  $\rho$  is the atomic density of the condensate,  $\Delta = \omega_p - \omega_{31}$  is the frequency detuning of the probe field with frequency  $\omega_p$  from the resonant electronic transition  $\omega_{31}$ ,  $\Gamma_2$  and  $\Gamma_3$  respectively denote the dephasing rates of the atomic coherences of the lower states,  $\mu_{31} = 3\varepsilon_0 \hbar \lambda_{31}^2 \gamma / 8\pi^2$  is the dipole matrix element between upper state  $|3\rangle$  and lower state  $|1\rangle$ , involved in the probe transition with  $\lambda_{31}$  being the resonant wavelength of the probe transition and  $\gamma$  being the radiation decay rate between  $|3\rangle$  and  $|1\rangle$ . For the cold gases considered in this paper and assuming co-propagating laser beams, Doppler shift in the detuning is neglected.

At the probe resonance, imaginary part of  $\chi$  becomes negligible and results in turning an optically opaque medium transparent. Furthermore, EIT can be used to achieve ultra-slow light velocities, owing to the steep dispersion of the EIT susceptibility  $\chi$  about the probe resonance [14].

### 3. Our proposed scheme of pulse amplifier

A schematic of the proposed BEC pulse amplifier is shown in Fig. 1. The short cavity, initially extending from the output coupler (OC) up to the end high reflector (HR<sub>1</sub>), contains a gain medium and is first passively mode-locked by using the technique of Kerr lens mode locking or a saturable absorber [4]. The cavity is then extended by removing HR<sub>1</sub> and two different BECs are introduced inside the resonator which now extends from OC up to the end high reflector HR<sub>2</sub>.

Although there is some interest to examine Josephson coupled BECs in optical cavities [28], here we assume the BECs are spatially disconnected, such that the condensates are kept in traps which are sufficiently far apart from each other to avoid spatial overlap of condensate wave functions. As long as there is Josephson coupling then condensate numbers would have dynamics and our treatment with frozen density profile cannot be applied. In addition to Josephson effect one could consider dense condensates with interaction terms and dissipation effects to find equilibrium density profiles so that our treatment can be extended to such a case to determine electric susceptibility for calculating possibility of dispersion compensation and reduction of group velocity.

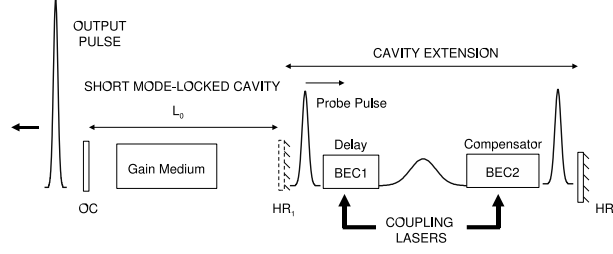


**Figure 1.** Schematic of a mode-locked laser cavity containing two Bose-Einstein condensates to reduce the pulse repetition rate and to compensate for dispersion. BEC1 introduces delay to lower the repetition rate and scales up the pulse energy.

The BECs are in the EIT configuration used in ultraslow light experiments [13, 29]. The circulating laser pulse acts as the probe field in the BECs and external coupling lasers are used to achieve transparency. BEC1 introduces delay to lower the repetition rate while the BEC2 acts as a dispersion compensator. Additional delay is also produced by BEC2. Axial sizes of the BECs are assumed to be sufficiently shorter than the cavity length while we have assumed that proper focusing optics is employed to keep the spotsize within the extent of the BEC, so that the original mode structure was preserved. Recent experiments with BECs in optical cavities [30] are successfully modeled under the assumption of frozen spatial mode profile of the cavity.

Let us assume that the repetition rate of the short cavity is  $f_0 = c/2L_0$ , where  $L_0$  is the effective optical path length of the short resonator. In the simulations, we assumed that, without the intracavity BECs,  $f_0 = 25$  MHz which is easily achievable in standard mode-locked laser configurations. The total round-trip group delay  $T_g$  (in other words, the reverse of the reduced pulse repetition rate) will be given by

$$T_g = 2 \left( \frac{L_1}{v_{g1}} + \frac{L_2}{v_{g2}} \right). \quad (2)$$

Here, we neglected the round-trip group delay of the initial short cavity, and denoted the effective length and the group velocity for the condensates ( $i = 1, 2$ ) as  $L_i$  and  $v_{gi}$ , respectively, such that [16],

$$L_i = \left[ \frac{4\pi}{N} \int_0^\infty r dr \int_0^\infty z^2 \rho_i(r, z) dz \right]^{1/2} \quad (3)$$

and

$$\frac{1}{v_{gi}} = \frac{1}{c} + \frac{\pi}{\lambda} \frac{\partial \chi_i}{\partial \Delta}. \quad (4)$$

The effective length is the rms width of the density distribution of the condensate along the cavity axis ( $z$ ). Here  $r$  is the radial coordinate. In the ideal case, where the inclusion of the BECs add no loss to the resonator, the average output power of the laser remains nearly equal to that of the short cavity. During mode-locked operation

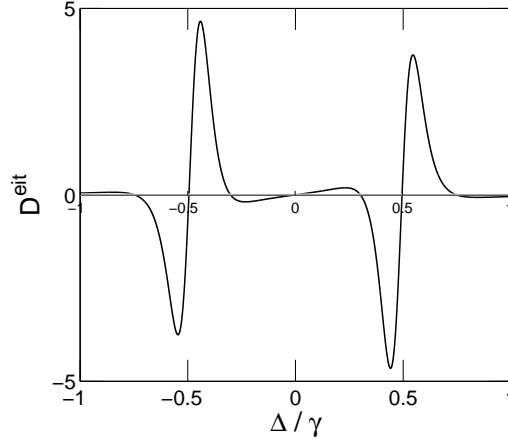


**Figure 2.** Dispersion coefficient for EIT in a BEC of  $^{23}\text{Na}$  atoms, at temperature  $T = 381$  nK, with parameters [13],  $M = 23$  amu,  $a_s = 2.75$  nm,  $N_1 = N_2 = 8.3 \times 10^6$ ,  $\omega_r = 2\pi \times 69$  Hz,  $\omega_z = 2\pi \times 21$  Hz,  $\Gamma_3 = 0.5\gamma$ ,  $\gamma = 2\pi \times 10.01$  MHz, and  $\Gamma_2 = 2\pi \times 10^3$  Hz. Resonance wavelength for the probe laser transition is  $\lambda = 589$  nm. We take  $\Omega_c = 2.5\gamma$ . The peak density is  $\rho_{peak} = 6.87 \times 10^{19}$  ( $1/\text{m}^3$ ).  $D$  is normalized by  $1/10^{-10}$  ( $\text{sec}^2$ ). Though it is not visible in the figure,  $D(0) = 2.7 \times 10^{-20}$  ( $\text{sec}^2$ ). At the operating point of the amplifier,  $\Delta = -0.01\gamma$ , we find  $D = 7.9 \times 10^{-13}$   $\text{sec}^2$ .

of the extended cavity, the amplification factor  $A$  for the pulse energy will therefore be given by  $A = T_g f_0$ .

## 4. Results

We consider two BECs of  $^{23}\text{Na}$  atoms with parameters [13],  $M = 23$  amu,  $a_s = 2.75$  nm,  $N_1 = N_2 = 8.3 \times 10^6$ ,  $\omega_r = 2\pi \times 69$  Hz,  $\omega_z = 2\pi \times 21$  Hz,  $\Gamma_3 = 0.5\gamma$ ,  $\gamma = 2\pi \times 10.01$  MHz, and  $\Gamma_2 = 2\pi \times 10^3$  Hz. Resonance wavelength for the probe laser transition is  $\lambda = 589$  nm. We take  $\Omega_c = 2.5\gamma$  and  $\Delta_1 = 0.01\gamma$ .

### 4.1. Dispersion compensation

Within the transparency window of EIT, imaginary part of the susceptibility ( $\chi''$ ) is very small compared to the real part of the susceptibility ( $\chi'$ ). The group velocity dispersion  $D_i$  is given by  $D_i = d^2\phi_i/d\omega^2$  [31], where  $\phi_i = n_i\omega L_i/c$  is the accumulated phase, with  $n_i$  being the refractive index. Using  $n_i = \sqrt{1 + \chi_i} \approx 1 + \chi_i/2$ ,  $D_i$  can be expressed as

$$D_i = \frac{L_i}{c} \left( \frac{d\chi_i}{d\omega} + \frac{\omega}{2} \frac{d^2\chi_i}{d\omega^2} \right). \quad (5)$$

In the proposed scheme, the second order dispersion of the BEC1 is positive for a probe pulse slightly blue detuned from the resonance, which can be seen in Fig. 2.

At the same but red detuning, dispersion would be almost the same, but with the opposite sign. For propagation through a single BEC, this sign change is not relevant

on pulse broadening. On the other hand, by introducing a second BEC, plays a role through the pulse chirp. The pulses emerging from BEC1 are broadened and chirped. In other words, the instantaneous carrier frequency differs across the temporal pulse profile from the central carrier frequency. In the presence of second-order group velocity dispersion, this chirp is approximately linear near the pulse center. If the chirped pulse then enters the second BEC whose group velocity dispersion parameter is adjusted to be equal in magnitude but opposite in sign to that of BEC1, the linear chirp near the pulse center will be cancelled and the initial pulsewidth will be restored (see Refs. [31, 32] and references therein). For that aim, we assume that BEC2 is also in an EIT configuration but energy levels for the probe transition are shifted by an external magnetic field. Hence the blue detuned probe for BEC1 would be red detuned for BEC2 by the same amount. As the dispersions are of the same magnitude but of opposite sign, this can be used to compensate for the positive dispersion of the delay segment (BEC1), provided that the dispersion introduced in the other intracavity elements are negligible.

To determine the operating point of the amplifier, we adjust the parameters of the BECs so that  $D^{BEC1}(x_1) + D^{BEC2}(x_2) = 0$  where  $x_1 = \Delta_1/\gamma, x_2 = \Delta_2/\gamma$ . The operating point would be independent of temperature for identical condensates as  $D_i$  are proportional to the  $\rho_i L_i$  that are the same for both BECs. Dependence of  $D$  on  $\Delta$  is shown in Fig. 2 at the chosen temperature of  $T = 381$  nK. We find that dispersion compensation condition,  $D_1 = -D_2$ , is satisfied by  $x_1 = -x_2$  at  $\Delta_1/\gamma = 0.01$  which will be the operating point of the amplifier.

We assumed identical traps and condensates only for the sake for simplicity. The main formalism and the dispersion compensation condition  $D_1 = -D_2$  is generally valid for non-identical traps and condensates. The effect of different number of atoms in the BECs would be on the operating point (detuning of the probe field) where the dispersion compensation is achieved. We can make a simple estimate. Dispersion coefficient is proportional to the product of BEC density and length, both of which are related to the chemical potential by power laws. Thus the ratio  $D_1/D_2$  is related to the ratio of the chemical potentials of the BECs. Assuming Thomas-Fermi profiles,  $D_1/D_2$  has negligibly weak temperature dependence, but strong dependence on the ratio of condensed particle numbers  $N_1/N_2$ . If we know  $N_1$  and  $N_2$  then the operating point can be determined by simple calculation. Due to number fluctuations the compensation of the dispersion would be incomplete. However, the amplification factors are modest in our case and the pulse duration is in the order of microseconds. For such pulses the dispersion is not too strong and even partial compensation of dispersion should be sufficient and thus we can say fluctuation of particle number would not have crucial effects on our conclusions.

#### 4.2. Heating rate

The heating rate of a gaseous sample due to optical absorption is a standard problem in laser cooling theory (see e.g. [33] (chapter 4)). The rate of change in the average

kinetic energy of an atom due to absorption can be evaluated from

$$\frac{1}{2m} \frac{d\bar{p}^2}{dt} = vF_{rad}, \quad (6)$$

where  $v = \hbar k_L/m$  is the recoil velocity of the atom with mass  $m$  due to absorption of a laser photon at wave number  $k_L$ , and  $F_{rad}$  is the radiation force acting on the atom. Impulse-momentum theorem can be written for the absorption as  $F_{rad}\tau_{rad} = \hbar k_L$ , where  $\tau_{rad}$  is the characteristic time of interaction between the atom and the radiation field. Introducing  $\Gamma_{rad} = 1/\tau_{rad}$ , we rewrite the relation as  $F_{rad} = \hbar k_L \Gamma_{rad}$ . Second-order perturbation theory can be used to find  $\Gamma_{rad}$ . Analogous to ac Stark shifts, we write the energy level shift as  $\Delta E = -\frac{1}{2}\alpha\langle\mathcal{E}^2\rangle$  where  $\alpha$  is the single-atom complex polarizability and  $\mathcal{E}$  is the laser pulse amplitude. Imaginary part of the level shift can be identified by  $\Gamma_{rad} = -(2/\hbar)Im(\Delta E) = \alpha''\langle\mathcal{E}^2\rangle/\hbar$ . This yields

$$F_{rad} = \frac{1}{\hbar}(\hbar k_L)\alpha''\langle\mathcal{E}^2\rangle. \quad (7)$$

In our case,  $\alpha = \mu_{31}^2 L(\Delta)/\hbar$  is the single atom EIT susceptibility, where we introduced a notation

$$L(\Delta) = \frac{i(-i\Delta + \Gamma_2/2)}{(\Gamma_2/2 - i\Delta)(\Gamma_3/2 - i\Delta) + \Omega_C^2/4}. \quad (8)$$

The average rate of change of kinetic energy due to absorption then becomes

$$\frac{1}{2m} \frac{d\bar{p}^2}{dt} = \frac{2}{2m}(\hbar k_L)^2 \frac{\mu_{31}^2\langle\mathcal{E}^2\rangle}{\hbar^2} L''(\Delta), \quad (9)$$

where  $L''(\Delta)$  is the imaginary part of  $L(\Delta)$ . Identifying the probe Rabi frequency as  $\Omega_p^2 = \mu_{31}^2\langle\mathcal{E}^2\rangle/\hbar^2$ , and by using the equipartition theorem,  $k_B T/2 = \bar{p}^2/2m$ , we finally get the heating rate  $\kappa$  to be

$$\kappa = \frac{dT}{dt} = \frac{4}{mk_B}(\hbar k_L)^2 \Omega_p^2 L''(\Delta). \quad (10)$$

An additional factor of 2 is introduced to take into account subsequent emission and absorption processes together. For the parameters we use in our simulations, taking  $\Omega_p = 0.1\Omega_c$ , the heating rate is evaluated to be  $\kappa \sim 1.6$  mK/sec. We do not assume zero temperature BECs. The heating rate  $\kappa$ , or the rate of loss of condensed particles, exhibit linear dependence with the temperature and thus one can always choose the initial time ( $t_0$ ) corresponding to the initial temperature ( $T_0$ ) by  $t_0 = T_0/\kappa$  so that  $T = \kappa t$ . We report our results in the figures as functions of temperature which can be translated to time dependence by this scaling transformation. The effect of dynamically changing temperature  $T = \kappa t$  is to make the density of the cloud time dependent. We shall use semi-ideal model of the BEC [34] for an analytical expression of the density of the atomic cloud.

Indeed the main dissipation channel is the loss of the condensate atoms. In addition to heating, other mechanisms of condensed particle loss may occur, such as three-body loss [35]. Here we do not take them into account as we assume BECs are sufficiently dilute, and the number of particles are not too large. Thus in our case the only source



of particle loss out of the condensate is heating, or the recoil momentum transfer, by pulse absorption. Atoms with sufficient recoil are thermalized and removed from the condensate phase. This in turn reduces the density of the condensate. Once the density becomes lower than the critical density required to maintain the condensate, then the condensate is destroyed and the gas is entirely thermalized. The semi-classical model we employ is in fact is to treat such a case. It contains both the thermal and condensate phases. Below the critical temperature thermal phase serves as the thermal background for the dominant condensate phase. Electromagnetically induced transparency has normally negligible absorption but still it is not zero. Single pulse would transfer a little energy to the condensate. Duration of the interaction due to pulse delay is less than the time needed to transfer sufficient energy to destroy the condensate. The recoil energy or the received kinetic energy is translated in our treatment to the temperature variable. Temperature and time has linear relation. The loss of the atoms out of the condensate phase or the condensate fraction reduces by the temperature. These arguments can be put into mathematical context using the semi-ideal model as follows.

The total density at a temperature  $T(t)$  is then written to be

$$\rho(\vec{r}, t) = \frac{\mu(t) - V(\vec{r})}{U_0} \Theta(\mu(t) - V(\vec{r})) \Theta(T_C - T(t)) + \frac{g_{3/2}(ze^{-\beta V})}{\lambda_T(t)^3}, \quad (11)$$

where  $U_0 = 4\pi\hbar^2 a_s/m$ ;  $m$  is atomic mass;  $a_s$  is the atomic s-wave scattering length;  $\mu$  is the chemical potential;  $\Theta(\cdot)$  is the Heaviside step function;  $g_n(x) = \sum_j x^j/j^n$  is the Bose function;  $\lambda_T$  is the thermal de Bröglie wavelength;  $\beta = 1/k_B T$ ;  $z = \exp(\beta\mu)$  is the fugacity, and  $T_C$  is the critical temperature which is  $T_C = 424$  nK in our case. The optical pulse would heat the cloud to  $T_C$  in  $265 \mu\text{s}$ . The maximum pulse delay time  $\sim 65 \mu\text{s}$  is less than the critical time at which the condensate turns into thermal gas. However, as the multiple passes of the pulse train over the condensate continue to heat it we shall consider time, and corresponding temperature range, in our examinations beyond the critical time and temperature. The external trapping potential is  $V(\vec{r}) = (m/2)(\omega_r^2 r^2 + \omega_z^2 z^2)$  with  $\omega_r$  the radial trap frequency and  $\omega_z$  the angular frequency in the  $z$  direction.  $\mu$  is determined from  $N = \int d^3\vec{r} \rho(\vec{r})$ . At temperatures below  $T_c$  this yields[34]

$$\mu(t) = \mu_{TF} \left( \frac{N_0}{N}(t) \right)^{2/5}, \quad (12)$$

where  $\mu_{TF}$  is the chemical potential evaluated under Thomas-Fermi approximation and the condensate fraction is given by

$$\frac{N_0}{N}(t) = 1 - x(t)^3 - s \frac{\zeta(2)}{\zeta(3)} x(t)^2 (1 - x(t)^3)^{2/5}, \quad (13)$$

with  $x(t) = T(t)/T_c$ , and  $\zeta$  is the Riemann-Zeta function. Thomas-Fermi profile is valid for small healing length,  $\xi = 1/\sqrt{8\pi a_s \rho}$ , of the condensate relative to the harmonic trap length. The scaling parameter  $s$ , characterizing the strength of atomic interactions

within the condensate, is calculated to be [34]

$$s = \frac{\mu_{TF}}{k_B T_C} = \frac{1}{2} \zeta(3)^{1/3} \left( 15 N^{1/6} \frac{a_s}{a_h} \right)^{2/5}. \quad (14)$$

Here,  $a_h = \sqrt{\hbar/m(\omega_z \omega_r^2)^{1/3}}$  denotes the average harmonic oscillator length scale. At temperatures above  $T_C$ ,  $\mu$  can be determined from  $\text{Li}_3(z) = \zeta(3)/x^3$ , where  $\text{Li}_3(\cdot)$  is the third-order polylogarithm function. The semi-ideal model has a wide-range of validity in representing density distribution of a trapped Bose gas at finite temperature provided that  $s < 0.4$  [34]. At the same time, the interactions are assumed to be strong enough to ensure  $\mu \gg \hbar\omega_{r,z}$ , so that the kinetic energy of the condensate can be neglected according to the Thomas-Fermi approximation. In typical slow-light experiments in cold atomic gases,  $s$  remains within these limits. The time dependence of the density is translated to the condensate expansion and the group velocity increase which in turn affects the amplification factor as shown in the following section. We note that decoupling of the matter wave dynamics from the optical pulse dynamics is based upon their significantly different time scales. The dynamics of condensate matter wave happens in the  $ms$  scale, while optical pulse evolves in  $\mu s$  [36]. We also ignore higher dimensional propagation effects in the optical pulse dynamics such as multimode waveguiding [37] and diffraction losses [38].

### 4.3. Amplification factor

The result of the temperature dependent amplification calculations is shown in Fig. 3. Amplification factor increases with temperature up to a temperature  $T \sim 318$  nK, close but less than the critical temperature  $T_C = 424$  nK of the BEC. In the semi-ideal picture of the condensate density profile, this is due to the contribution from the increasing effect of the thermal component in the pulse propagation via the group velocity and the length of the condensate.

As can be seen in Fig. 4, the group velocity weakly depends on the temperature in the condensate phase. Thermal behavior of the group velocity can be explained by examining the thermal behavior of the condensate density. In the semi-ideal model that we use both the condensate and the thermal gas components are considered. Below the critical temperature, the condensate component emerges sharply and dominates over the thermal background gas. Density varies little at low temperatures. Thus the ultraslow propagation speeds weakly change with the temperature. After the critical temperature, there is no more condensate and the thermal gas gets more rapidly diluted with the temperature, causing the kink in Fig. 4(a), which is also observed experimentally [13].

The main effect of the temperature is the expansion of the condensate which causes the increase of the delay times of the pulse through the condensate and hence  $T_g$  increases. Behavior of the amplification factor with the temperature follows that of the effective length. Beyond  $T_c$ , almost linear behavior of group velocity and the effective length with temperature result in weak dependence of  $T_g$  and hence amplification on the temperature. The amplification is larger in the condensation regime due to large

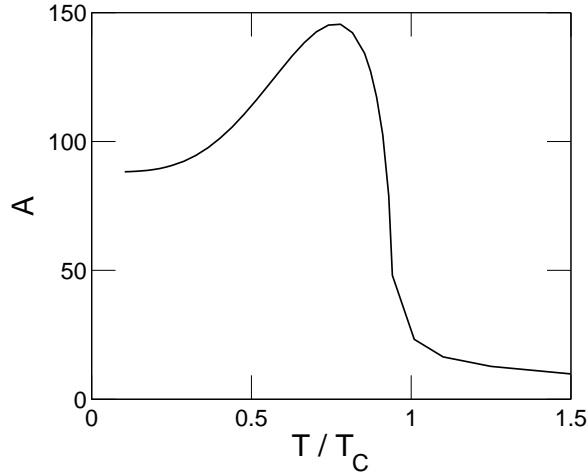


**Figure 3.** Dependence of amplification factor  $A$  on temperature, for the same parameters as in Fig. 2. The temperature is scaled by the critical temperature  $T_C = 424$  nK. The heating rate  $\kappa = 1.6$  mK/sec translates the same behavior into the time domain via  $T = \kappa t$ .

group delays. Fig. 4(a) shows that group velocity of the pulse in the thermal gas regime rises sharply and it is faster than expansion of the atomic cloud shown in Fig. 4(b). Accordingly, amplification factor sharply drops after a critical temperature close to  $T_c$  and continues to decrease slowly in the thermal gas phase.

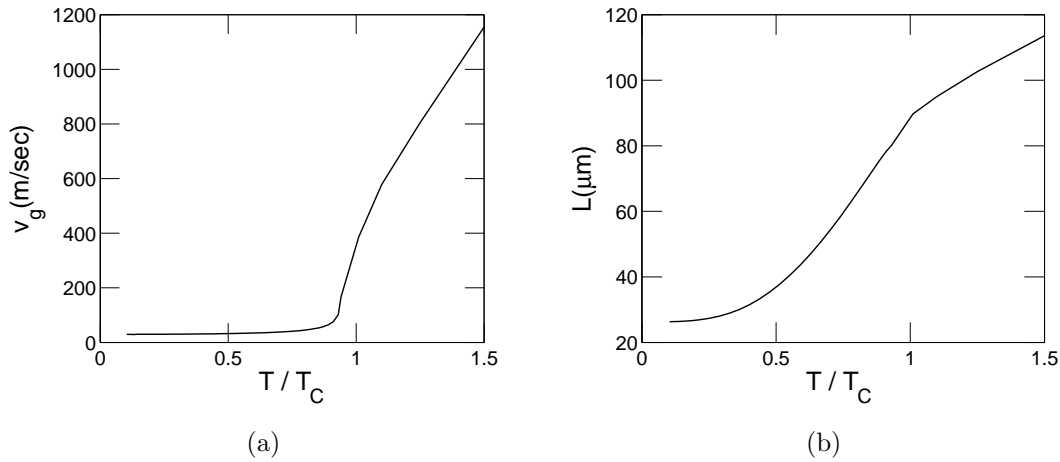


**Figure 4.** (a) Thermal behavior of the group velocity of the probe pulse. (b) Thermal behavior of the effective length of the BEC. The parameters used for both curves are the same as in Fig. 2. The temperature is scaled by the critical temperature  $T_C = 424$  nK. The heating rate  $\kappa = 1.6$  mK/sec translates the same behaviors into the time domain via  $T = \kappa t$ .

#### 4.4. Spectral bandwidth

Finally, we investigate the spectral bandwidth limitations of the BEC. Ideally, it is desirable to have a system which has a very broad transparency to support the propagation of pulses with very short duration. To provide a feel for how short a pulse the BECs can support, we calculate the spectral bandwidth  $\Delta\nu$  that corresponds to the transparency window of the BEC in the EIT scheme. The net bandwidth due to both of the BECs is  $2\Delta\nu$  so that the temporal width  $\tau_p$  of the pulse that can be supported can be estimated by  $\tau_p = 1/2\Delta\nu$ . Using [10]

$$\Delta\nu = \frac{\Omega_c^2}{\gamma} \frac{1}{\sqrt{\kappa_\nu}}, \quad (15)$$

with  $\kappa_\nu = 3\rho\lambda^3(k_L L)/8\pi^2$  being the opacity of the atomic cloud of length  $L$  and density  $\rho$ , we find  $\Delta\nu \sim 0.1\gamma$ . Note that the operation point  $\Delta = 0.01\gamma$  lies within the transparency window. The pulses that can be supported by the condensates should have widths of the order of  $\sim \mu\text{s}$ . Pulses of shorter widths could be supported by considering larger  $\Omega_c$ . The cost however would be to get lower amplification factors as the group velocity would increase with increasing Rabi frequency of the control field. More ingenious designs that specifically considers transparency window enhancement for broadband pulses are proposed [39] but their integration to the present proposal require further studies.

## 5. Conclusions

In conclusion, we have investigated the feasibility of using Bose-Einstein condensates for laser pulse amplification. The method involves the introduction of two BECs inside the resonator of a passively mode-locked laser. The large delay produced by the BECs lowers the pulse repetition rate and scales up the output energy. Our calculations show that pulse amplification factors of the order  $\sim 10^2$  should be possible over a condensate length of  $\sim 50 \mu\text{m}$ . We further showed that a second BEC could be used to provide dispersion compensation. However, the amplification factor decreases with time due to the presence of optical absorption. We have estimated the heating rate to be about 1.6 mK/sec, which severely limits the operation time of the system in the condensate regime. A critical time of operation for optimum amplification is found to be about 200  $\mu\text{s}$ . That would require an additional optical switching to extract the pulse at the right time out of the cavity. Alternatively, reducing the effects of absorption by considering multi-level EIT systems [40, 41] or designing a compensating simultaneous cooling mechanism on the atomic cloud in EIT scheme [42, 43] can be considered. This would eliminate the need of reconstruction of the BEC to amplify different pulses at optimum conditions. For quick and easy generation of BECs atom chips can be promising [44]. To aim at higher intensities and amplification factors, the nonlinear response of the atomic gas should also be taken into account. Denser condensates, with nonlinear response and quantum corrections, including atom-atom interactions, but without local field correction, seem

to be beneficial for larger delay times as well [15].

## Acknowledgments

D.T. acknowledges the support from TUBITAK (The Scientific and Technological Research Council of Turkey) Career Grant No 109T686. Ö. E. M. is supported by TUBITAK under project TBAG-109T267. D. T. thanks G. S. Agarwal for helpful discussions.

## References

- [1] G.J. Tearney, M.E. Brezinski, B.E. Bouma, S.A. Boppart, C. Pitris, J.F. Southern, and J.G. Fujimoto. In vivo endoscopic optical biopsy with optical coherence tomography. *Science*, 276(5321):2037, 1997.
- [2] M. Drescher, M. Hentschel, R. Kienberger, M. Uiberacker, V. Yakovlev, A. Scrinzi, T. Westerwalbesloh, U. Kleineberg, U. Heinzmann, and F. Krausz. Time-resolved atomic inner-shell spectroscopy. *Nature*, 419(6909):803–807, 2002.
- [3] Ch. Spielmann, N. H. Burnett, S. Sartania, R. Koppitsch, M. Schnürer, C. Kan, M. Lenzner, P. Wobrauschek, and F. Krausz. Generation of coherent x-rays in the water window using 5-Femtosecond laser pulses. *Science*, 278(5338):pp. 661–664, 1997.
- [4] H.A. Haus. Mode-locking of lasers. *Selected Topics in Quantum Electronics, IEEE Journal of*, 6(6):1173–1185, 2000.
- [5] SH Cho, BE Bouma, EP Ippen, and JG Fujimoto. Low-repetition-rate high-peak-power kerr-lens mode-locked tial laser with a multiple-pass cavity. *Optics Letters*, 24(6):417–419, 1999.
- [6] S. Naumov, A. Fernandez, R. Graf, P. Dombi, F. Krausz, and A. Apolonski. Approaching the microjoule frontier with femtosecond laser oscillators. *New Journal of Physics*, 7:216, 2005.
- [7] A. Sennaroglu, O. E. Mustecaplioglu, and D. Tarhan. Laser pulse amplification with Bose-Einstein condensates. E-Print, ArXiv: 0707.0145v2, 2007.
- [8] S.E. Harris. Electromagnetically induced transparency. *Physics Today*, 50:36, 1997.
- [9] JP Marangos. Electromagnetically induced transparency. *Journal of Modern Optics*, 45(3):471–503, 1998.
- [10] M. Fleischhauer, A. Imamoglu, and J.P. Marangos. Electromagnetically induced transparency: Optics in coherent media. *Reviews of Modern Physics*, 77(2):633, 2005.
- [11] MD Lukin, PR Hemmer, and MO Scully. Resonant nonlinear optics in phase-coherent media. *Advances in Atomic, Molecular, and Optical Physics*, 42:347–386, 2000.
- [12] Hai Wang, D. J. Goorskey, W. H. Burkett, and Min Xiao. Cavity-linewidth narrowing by means of electromagnetically induced transparency. *Optics Letters*, 25(23):1732–1734, December 2000.
- [13] L.V. Hau, S.E. Harris, Z. Dutton, and C.H. Behroozi. Light speed reduction to 17 metres per second in an ultracold atomic gas. *Nature*, 397(6720):594–598, 1999.
- [14] C. Liu, Z. Dutton, C.H. Behroozi, and L.V. Hau. Observation of coherent optical information storage in an atomic medium using halted light pulses. *Nature*, 409(6819):490–493, 2001.
- [15] Z. Haghshenasfard and M.G. Cottam. Controlling the repetition rate of a mode-locked laser using an f-deformed Bose–Einstein condensate. *Journal of Physics B: Atomic, Molecular and Optical Physics*, 45:025501, 2012.
- [16] D. Tarhan, A. Sennaroglu, and Ö. E. Müstecaplioglu. Dispersive effects on optical information storage in Bose-Einstein condensates with ultraslow short pulses. *JOSA B*, 23(9):1925–1933, 2006.
- [17] Donald R. Herriott and Harry J. Schulte. Folded optical delay lines. *Applied Optics*, 4(8):883–889, August 1965.

- [18] A. Sennaroglu, Jr. Kowalewicz, A.M., E.P. Ippen, and J.G. Fujimoto. Compact femtosecond lasers based on novel multipass cavities. *IEEE Journal of Quantum Electronics*, 40(5):519 – 528, May 2004.
- [19] MO Scully and MS Zubairy. *Quantum Optics*. Cambridge University Press, Cambridge, 1997.
- [20] S. Wielandy and A.L. Gaeta. Investigation of electromagnetically induced transparency in the strong probe regime. *Physical Review A*, 58(3):2500, 1998.
- [21] SE Harris and Z.F. Luo. Preparation energy for electromagnetically induced transparency. *Physical Review A*, 52(2):928–931, 1995.
- [22] A. Kasapi, M. Jain, GY Yin, and SE Harris. Electromagnetically induced transparency: propagation dynamics. *Physical review letters*, 74(13):2447–2450, 1995.
- [23] R. Grobe, FT Hioe, and JH Eberly. Formation of shape-preserving pulses in a nonlinear adiabatically integrable system. *Physical review letters*, 73(24):3183–3186, 1994.
- [24] Y. Li and M. Xiao. Enhancement of nondegenerate four-wave mixing based on electromagnetically induced transparency in rubidium atoms. *Optics letters*, 21(14):1064–1066, 1996.
- [25] BS Ham, MS Shahriar, and PR Hemmer. Enhanced nondegenerate four-wave mixing owing to electromagnetically induced transparency in a spectral hole-burning crystal. *Optics letters*, 22(15):1138–1140, 1997.
- [26] SE Harris and M. Jain. Optical parametric oscillators pumped by population-trapped atoms. *Optics letters*, 22(9):636–638, 1997.
- [27] GZ Zhang, DW Tokaryk, BP Stoicheff, and K. Hakuta. Nonlinear generation of extreme-ultraviolet radiation in atomic hydrogen using electromagnetically induced transparency. *Physical Review A*, 56(1):813, 1997.
- [28] J. M. Zhang, W. M. Liu, and D. L. Zhou. Mean-field dynamics of a bose josephson junction in an optical cavity. *Physical Review A*, 78(4):043618, October 2008.
- [29] A.B. Matsko, O. Kocharovskaya, Y. Rostovtsev, G.R. Welch, A.S. Zibrov, and M.O. Scully. Slow, ultraslow, stored, and frozen light. *Advances in atomic, molecular, and optical physics*, 46:191–242, 2001.
- [30] Kristian Baumann, Christine Guerlin, Ferdinand Brennecke, and Tilman Esslinger. Dicke quantum phase transition with a superfluid gas in an optical cavity. *Nature*, 464(7293):1301–1306, April 2010.
- [31] A. Sennaroglu. *Photonics and Laser Engineering: Principles, Devices, and Applications*. McGraw-Hill Professional, 1 edition, May 2010.
- [32] A. Sennaroglu. Broadly tunable cr<sup>4+</sup>-doped solid-state lasers in the near infrared and visible. *Progress in Quantum Electronics*, 26(6):287–352, November 2002.
- [33] C. J Pethick and H. Smith. *Bose-Einstein Condensation in Dilute Gases*, volume 1. Cambridge University Press, December 2001.
- [34] M. Naraschewski and D. M. Stamper-Kurn. Analytical description of a trapped semi-ideal bose gas at finite temperature. *Physical Review A*, 58(3):2423–2426, 1998.
- [35] Yeong E. Kim and Alexander L. Zubarev. Three-body losses in trapped bose-einstein-condensed gases. *Physical Review A*, 69(2):023602, February 2004.
- [36] Z. Dutton and L.V. Hau. Storing and processing optical information with ultraslow light in bose-einstein condensates. *Phys. Rev. A*, 70(5):053831, November 2004.
- [37] Devrim Tarhan, Nazmi Postacioglu, and Özgür E. Müstecaplioğlu. Ultraslow optical waveguiding in an atomic bose-einstein condensate. *Opt. Lett.*, 32(9):1038–1040, May 2007.
- [38] Ö. E. Mustecaplioglu and L. You. Propagation of raman-matched laser pulses through a bose-einstein condensate. *Optics Communications*, 193:301 – 312, June 2001.
- [39] D. D. Yavuz. Electromagnetically induced transparency with broadband laser pulses. *Phys. Rev. A*, 75(3):031801, March 2007.
- [40] P. R. Hemmer, D. P. Katz, J. Donoghue, M. Cronin-Golomb, M. S. Shahriar, and P. Kumar. Efficient low-intensity optical phase conjugation based on coherent population trapping in sodium. *Optics Letters*, 20(9):982–984, May 1995.

- [41] J. Wang, L.B. Kong, X.H. Tu, K.J. Jiang, K. Li, H.W. Xiong, Yifu Zhu, and M.S. Zhan. Electromagnetically induced transparency in multi-level cascade scheme of cold rubidium atoms. *Physics Letters A*, 328(6):437–443, August 2004.
- [42] F. Schmidt-Kaler, J. Eschner, G. Morigi, C.F. Roos, D. Leibfried, A. Mundt, and R. Blatt. Laser cooling with electromagnetically induced transparency: application to trapped samples of ions or neutral atoms. *Applied Physics B: Lasers and Optics*, 73(8):807–814, 2001.
- [43] J Evers and C. H Keitel. Double-EIT ground-state laser cooling without blue-sideband heating. *Europhysics Letters (EPL)*, 68(3):370–376, November 2004.
- [44] W. Hänsel, P. Hommelhoff, T. W. Hänsch, and J. Reichel. Bose–Einstein condensation on a microelectronic chip. *Nature*, 413(6855):498–501, October 2001.